

Field orientation dependent decorrelation of magnetization reversal in uniaxial Co-films

J. A. Arregi, O. Idigoras, P. Vavassori, and A. Berger

Citation: *Appl. Phys. Lett.* **100**, 262403 (2012); doi: 10.1063/1.4730956

View online: <http://dx.doi.org/10.1063/1.4730956>

View Table of Contents: <http://apl.aip.org/resource/1/APPLAB/v100/i26>

Published by the [American Institute of Physics](http://www.aip.org).

Additional information on *Appl. Phys. Lett.*

Journal Homepage: <http://apl.aip.org/>

Journal Information: http://apl.aip.org/about/about_the_journal

Top downloads: http://apl.aip.org/features/most_downloaded

Information for Authors: <http://apl.aip.org/authors>

ADVERTISEMENT



AIP | Applied Physics Letters

Accepting Submissions in
Biophysics and Bio-Inspired Systems

Submit Today

AIP
Publishing

Field orientation dependent decorrelation of magnetization reversal in uniaxial Co-films

J. A. Arregi,^{1(a)} O. Idigoras,¹ P. Vavassori,^{1,2} and A. Berger¹

¹CIC nanoGUNE Consolider, Tolosa Hiribidea 76, E-20018 Donostia–San Sebastián, Spain

²IKERBASQUE, Basque Foundation for Science, E-48011 Bilbao, Spain

(Received 5 March 2012; accepted 8 June 2012; published online 26 June 2012)

Magnetization reversal correlation is studied as a function of the applied field angle for thin Co-films showing in-plane uniaxial magnetocrystalline anisotropy. We find that the field orientation angle has a profound effect onto the magnetization reversal process leading to a suppression of long-range correlation at sufficiently large field angles in the presence of grain alignment disorder. Correspondingly, this behavior allows for a tuning and the local confinement of magnetization reversal even in strongly exchange-coupled films and therefore presents a most desirable scenario for ultrahigh density magnetic recording. © 2012 American Institute of Physics. [<http://dx.doi.org/10.1063/1.4730956>]

Achieving a good understanding of magnetization reversal processes in magnetic materials is of fundamental importance and also of crucial significance in order to find novel solutions for device-oriented applications such as high-density magnetic recording.^{1–3} As information technology keeps increasing its demands on performance such as storage density⁴ and speed,⁵ simple down-scaling strategies are too limited and substantial further advances have to rely instead on entirely new phenomena, such as the present intensely studied spin transfer torque (STT).⁶ Hereby, it is also most important to have a deep insight into the underlying physical phenomena, including the properties of particle systems, such as granular^{7,8} or self-assembled⁹ materials, as well as determining the nature of the interactions within them.¹⁰ A key fundamental problem in conventional magnetic recording technology is related to the fact that recording media grains should be ferromagnetically coupled to fulfill stability requirements at small grain sizes.¹¹ However, one also needs individual grains to exhibit uncorrelated switching in order to advance the reduction of bit sizes, so that magnetically decoupled grains are the most desirable with respect to the writing process. Both these requirements for intergranular exchange coupling are generally considered to be fundamentally incompatible, because it is a materials property and thus, cannot be actively modified after the material has been fabricated. And even if some works have achieved a tuning of magnetization reversal correlation via temperature variation¹² and reprogrammable magnetic defect densities,¹³ these approaches seem unsuitable for an incorporation into conventional magnetic recording technology. In this work, we present a simple and temperature independent pathway to decorrelate magnetization reversal in exchange coupled thin magnetic films. Specifically, we demonstrate that a tuning of the applied field angle causes a most substantial variation of the magnetization reversal correlation length in partially epitaxial Co-films.

Several general considerations determine our sample selection. First, we want a sample type, in which long-range magnetization reversal correlation can occur as one extreme case of the tunable behavior. Thus, we utilize in-plane

magnetized films, so that the decorrelating influence of the magnetostatic interaction is suppressed. Second, we need an in-plane anisotropic sample to allow for angular dependent magnetic properties to occur. And lastly, we need sample types, in which the crystalline quality can be tuned easily while still preserving an anisotropic overall behavior, because it is known that magnetic films of very high crystalline order exhibit fully correlated magnetization reversal in a uniform field, independent of the magnetic field orientation.¹⁴

In order to fabricate suitable samples with uniaxial in-plane anisotropy and a notable level of disorder, we have grown 30 nm thick Co-films with an in-plane hexagonal closed-packed *c*-axis by sputter deposition on top of 25 nm thick Cr template layers onto *in situ* Ar-plasma cleaned Si(110) substrates. In a recent study, we have demonstrated that the crystalline quality as well as the magneto-crystalline anisotropy of such Co-films can be tuned in a reliable way by varying the Cr-based template layer and the Si-substrate preconditioning.^{14,15} We also deposited a 10 nm SiO₂ overlayer onto our samples in order to prevent them from oxidation. This methodology enabled us to vary the orientation ratio *OR*, defined as the ratio of easy axis to hard axis remanent magnetization, reliably in between 1 and 25.¹⁵ This quantity is generally determined by the applied field angle dependence of the remanent magnetization, as shown in the inset of Figure 1. In our studies of angular dependent magnetization reversal correlation, we found samples with *OR*-values of 5–10 most suitable. The value of the orientation ratio for the sample shown here is 7.1.

For the purpose of studying the evolution of the magnetization reversal correlation, angular dependent in-plane magnetic hysteresis loops were recorded by using a magneto-optical Kerr effect (MOKE) setup in longitudinal configuration. Figure 1 shows a schematic of the experimental configuration. In our setup, the sample is placed in between the electromagnet poles and held by a rotatable sample stage. Correspondingly, the magnetic field is applied at a variable angle θ with respect to the easy axis of the magnetization, which had been determined by measuring the

^{a)}Electronic email: j.arregi@nanogune.eu.

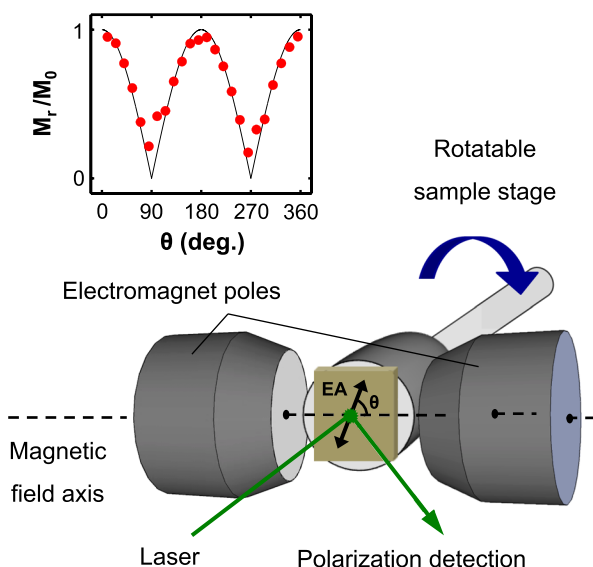


FIG. 1. Schematic of our experimental setup, which allows for an azimuthal sample rotation with respect to the applied magnetic field within the MOKE magnetometer. The in-plane applied field angle θ is defined with respect to the easy axis of the magnetization. The inset displays the angular dependence of the remanent magnetization normalized to the saturation value M_0 (dots) for one of our Co-film samples in comparison to the ideal Stoner-Wohlfarth single particle model (solid line).

angular dependent remanent magnetization (see inset in Figure 1). The angle θ is then changed with high resolution (down to a stepsize of only 0.2°) by rotating the sample holder stage in between recording subsequent hysteresis loops.

In contrast to standard MOKE-measurements of hysteresis loops, we performed here single-shot measurements of the magnetization reversal, rather than the conventional multi-loop averaging. This is of crucial importance for the reliability of our $M(H)$ data, because each data point corresponds to an individual magnetization state of the system rather than to an ensemble average. For the quality of our experiment, it is also important to record loops with high resolution in the applied field strength (0.1 Oe) in order to sample as many data points as possible near the switching field H_s , where the irreversible switching occurs. These experimental boundary conditions imply that a compromise must be found between the resolution level and the data acquisition speed in order to achieve a high signal-to-noise ratio and avoid signal drifts. In our measurements, we achieve single data point signal-to-noise ratios of up to 180 for acquisition times of 0.625 ms, using an overall sweep frequency of 0.8 Hz for the complete hysteresis loop.

Examples of our single shot hysteresis loop measurements for different applied field angles θ are shown in Figure 2. When the field is oriented close to the easy axis, such as in Figure 2(a), the hysteresis cycle shows a sample-sized magnetization jump of almost $2M_s$, resulting in a very rectangular hysteresis curve. The situation remains very similar in Figure 2(b), corresponding to $\theta = 20^\circ$, where the magnetization starts first reversing by coherent rotation, followed by a sample-sized magnetization avalanche. As the angle of the applied field is increased, we observe that above a certain threshold angle θ_c , intermediate states of the magnetization start to occur during the reversal, as is the case in Figure 2(c)

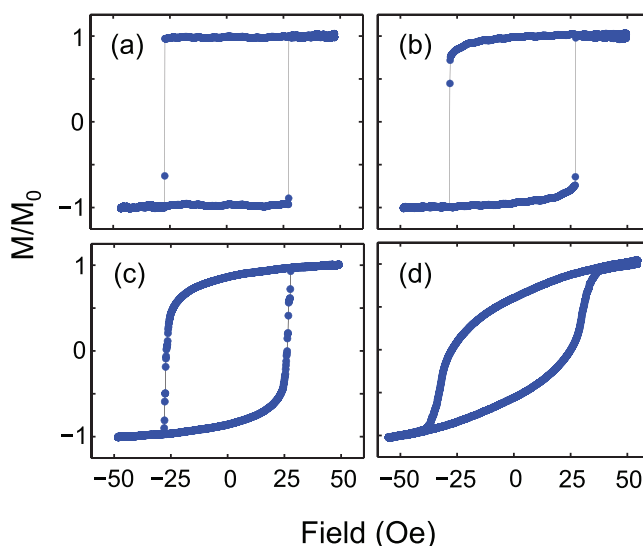


FIG. 2. Single-shot hysteresis loop measurements for a 30 nm thick Co-film, with the orientation of the applied field (a) along, (b) 20° away, (c) 35° away, and (d) 60° away from the easy axis. The solid line in each plot serves as a guide to the eye.

for $\theta = 35^\circ$. Upon further increasing the value of θ to 60° , shown in Figure 2(d), the $M(H)$ loop exhibits a completely smooth curve with no visible discontinuity. Thus, we observe a qualitative change of the reversal behavior upon increasing the magnetic field angle. When the field is oriented near the easy axis, reversal proceeds by means of correlated switching of nearly all grains, so that the system bypasses all intermediate magnetization states. In contrast to this fully correlated behavior, reversal occurs gradually for field angles above θ_c , with an apparently strongly reduced correlation length. Here, the reversal process is governed by domain nucleation, giving rise to stable and metastable states, in which the sample magnetization can take intermediate values.

For the purpose of corroborating the change in the lateral correlation length, we have investigated the micro-magnetic structures of our Co-films by means of Kerr microscopy. Figure 3 shows microscopy images of magnetization reversal states, i.e., the magnetic microstructure at H_s , for different angles of the applied field. The switching field H_s is defined by the maximum dM/dH , in contrast to the coercive field H_c which is nominally defined by a vanishing magnetization, i.e., $M = 0$. Depending on the sample orientation, H_c can be determined by reversible or irreversible magnetization reversal processes, while H_s is always defined by the irreversible switching processes. While trying to capture intermediate states of the magnetization for $\theta < \theta_c$, we only found uniform states just before and after switching occurs, as shown in Figure 3 for θ values of (a) 0° and (b) 5° . We occasionally acquired single snapshots showing intermediate magnetization states in the low angle regime, which are nonetheless consistent with the physical picture of a sample-sized magnetization reversal correlation. These specific pictures are generated by acquiring the magnetization value in the exact moment, in which the magnetization was reversing by means of a moving domain wall, so that we observe a transient magnetization state rather than a metastable intermediate state of the system. An example of

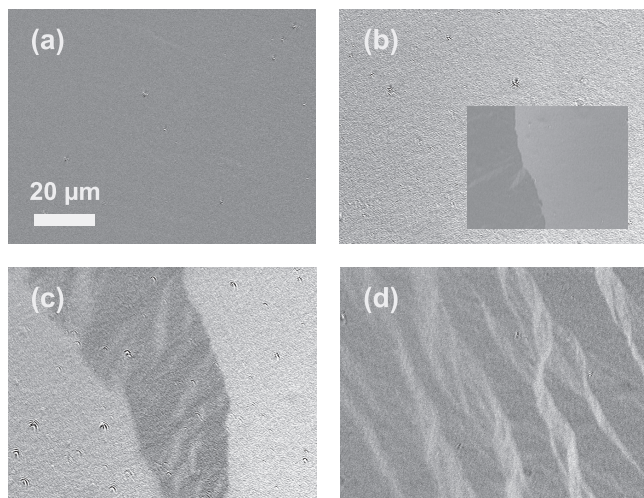


FIG. 3. Kerr microscopy images of a 30 nm thick uniaxial Co-film taken during magnetization reversal for different orientations of the applied field. The brightness is proportional to the local in-plane magnetization value. The orientation of the applied magnetic field is (a) along, (b) 5° away, (c) 30° away, and (d) 60° away from the easy axis. The inset in (b) shows an occasionally observed transient state in the same configuration as in the main image (b). The images were taken at magnetic field values of 27.3 Oe, 27.1 Oe, 26.3 Oe, and 25.1 Oe for image (a)–(d), respectively, which corresponds to $H = H_s$ for all field orientations.

these rarely observed transient states can be seen in the inset of the Figure 3(b). Such transient states are also occasionally visible in the hysteresis loops as, for example, in the decreasing field branches of the cycles in Figures 2(a) and 2(b). Besides the fact that these measured points are rare, they also vary strongly in their magnetization values from run to run, which is consistent with the fact that they are caused by transient states rather than originating from metastable intermediate states. Contrary to the behavior near the easy axis, images in Figures 3(c) and 3(d) present metastable multiple domain structures for θ equal to (c) 30° and (d) 60° . The figures thus demonstrate that the lateral correlation length decreases substantially to the point of suppressing long-range correlated switching. This introduces a qualitative change of the reversal mechanism, which is now governed by the formation of domains. While Figure 3(c) shows the co-existence of relatively large domains of up to $50 \mu\text{m}$ in size together with smaller domains, Figure 3(d) shows only smaller domains with sizes below $20 \mu\text{m}$. Thus, the correlation length of the reversal is further diminished upon increasing the magnetic field angle θ beyond the critical value, at which deviations from sample size correlations first occur.

Therefore, two different magnetization reversal modes exist in partially disordered thin Co-films with uniaxial anisotropy as a function of the applied field angle. For field orientations near the easy axis, the reversal occurs via a sample-sized magnetization jump, while the hysteresis loops are semi-continuous curves with multiple intermediate states for higher magnetic field angles. The existence of intermediate magnetization states and thus the corresponding reduction of the magnetization reversal correlation upon increasing the applied field angle θ is clearly visualized in Figure 4, where we represent complete magnetization reversal data sets as a function of field orientation θ and strength, given as normalized difference to the switching field H_s , by

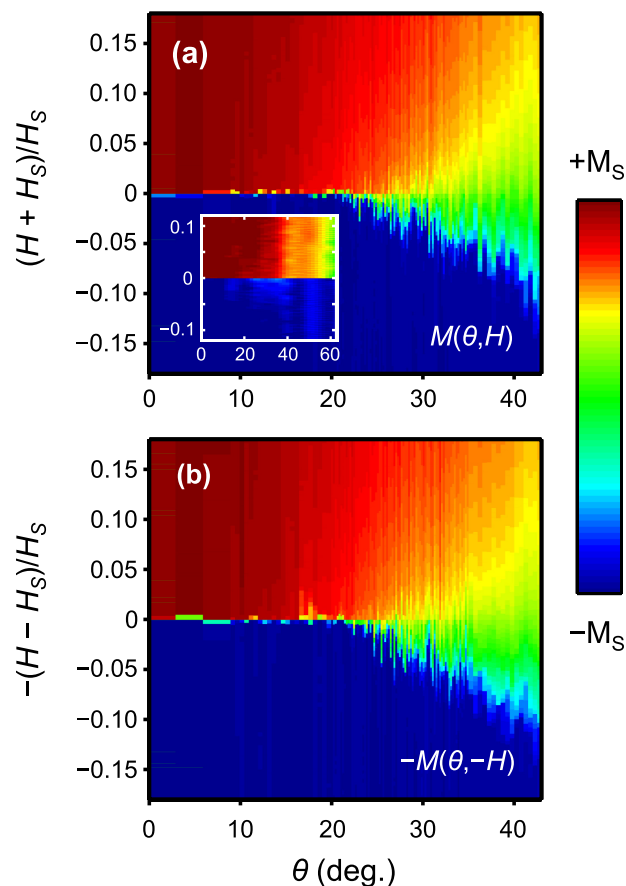


FIG. 4. Color-coded $M(\theta, H)$ magnetization maps for (a) the decreasing and (b) the increasing field branches of magnetic hysteresis loops in the vicinity of the magnetization reversal regime. The magnetization data are vertically centered and normalized by referencing the field values to the switching field H_s (which is defined as positive for both branches) for each hysteresis loop. The data in (b) have been plotted as $-M(\theta, -H)$ in order to make them visually comparable to the data in (a). The inset in (a) shows the $M(\theta, H)$ map for a Co-film with very high crystallographic order in comparison.

means of a color-coded magnetization map $M(\theta, H)$. Here, the two regions that exhibit the different reversal mechanisms are clearly distinguishable. At low values of θ up to approximately 23° for this specific sample, the hysteresis loop branches show an abrupt transition from positive (red) to negative (blue) saturation at the switching field, corresponding to the fully correlated magnetization reversal region. For field orientations $\theta > 23^\circ$, this phase separation line splits rather abruptly with the emergence of intermediate magnetization states, depicted as the green-colored regions, which grow in size as the applied field angle is moved further away from the easy axis. The data for the increasing field branch in (b) have been plotted as $-M(\theta, -H)$ to make use of the time reversal symmetry of the hysteresis loop so that the two data sets in (a) and (b) are directly comparable. Both data sets in Figure 4 display nearly identical results and are fully consistent with the physical picture of a qualitative change of the magnetization reversal mode at a distinct field orientation angle, which leads to the suppression of long-range magnetization reversal correlation on the high angle side. The small differences in the data sets shown in Figures 4(a) and 4(b) illustrate that there exists a measurement-to-measurement variation of the exact reversal point. This feature evidences that hysteresis loop averaging would

lead to an ensemble smoothing and consequently a loss of crucial individual reversal features of $M(H)$ data, which we avoided by means of our single shot measurements.

In our experiments, we find that this qualitative change is not observed in Co films with very high crystalline order. The magnetization map for such a sample ($OR = 25.1$) is shown in the inset of Figure 4(a). The gradual color change in the top part of the map from red to green reveals the magnetization rotation as the angle increases, but the transition at H_s stays abrupt for all θ values. This shows that even as magnetization rotation becomes more important for larger θ , the magnetization reversal is always fully correlated in highly ordered samples. The effect of magnetization rotation is also visible in Figures 4(a) and 4(b) as a gradual change of color for field values other than H_s . Nonetheless, this change is separate from the emergence of decorrelated reversal behavior at high angles. For samples that exhibit this qualitative change in magnetization reversal, we find that the critical angle θ_c varies from sample to sample in between 15° and 30° .

The observed behavior can be qualitatively understood in that by changing the applied field orientation, we change the effectiveness of the magnetic disorder that is present in the material due to the partial misalignment of the crystallographic grains. In particular, the role of the disorder is increasing as the field orientation is moving towards the hard axis, because the magnetic grains can better accommodate the changes in the external field by the magnetization rotation mechanism, and thus avoid the large buildup of Zeeman energy that happens along the easy axis. Correspondingly, the energy that is released upon the switching of a single grain for large θ is lower than for small θ , and also results in a smaller change of the effective inter-granular exchange field onto its neighbors. Thus, the exchange energy that tries to correlate the magnetization reversal of neighboring grains is weaker at larger θ . So, the disorder that is present in the Co-film, and which sets the energy barriers that the inter-granular exchange coupling has to overcome to achieve reversal correlation, becomes relatively more important at larger θ , and can therefore interrupt the grain-to-grain correlation of the reversal process. The relative energy balance between the correlating influence of the exchange coupling and the decorrelating effect of the disorder shifts as the applied field orientation is moved away from the easy axis of the system, and thus reduces the tendency of our films to show correlated reversal. We believe that this observation is of very substantial significance for perpendicular magnetic recording, for which recording media with large inter-granular exchange coupling are being utilized.^{16,17} Even though recording media generally have a very high degree of crystalline alignment,² they are exposed to a laterally inhomogeneous and non-collinear field pattern during the recording process. Thus, the core difference between our experiments and the magnetic recording scenario is that we use a laterally uniform magnetic field and a non-collinear arrangement of easy axes, while recording utilized laterally collinear easy axes media and non-collinear and inhomogeneous field pattern, such as the ones produced by trailing

shield or wrap-around shield write heads.¹⁷ In both cases, however, the competition between the aligning inter-granular exchange coupling strength and the decorrelating effect of the laterally varying field to easy axes angles are present and determine the lateral correlation length of the magnetization reversal. This analogy also explains, why an inclined magnetic recording field angle did not only improve the writability of individual grains, but also enabled the use of highly exchange coupled recording media,^{16,17} because at these high inclination field angles, magnetic reversal correlation can be more effectively suppressed, just as we demonstrated here with our experiments.

In conclusion, we demonstrated that the variation of the applied field angle causes a magnetization reversal mode transition from correlated behavior near the easy axis to uncorrelated reversal for orientations towards the hard axis. Hereby, we present a temperature independent pathway for the decorrelation of magnetization reversal in a single sample, an aspect that might be of crucial importance for ultra-high density magnetic recording.

We acknowledge funding from the Basque Government under the Etorrek Program Contract No. IE11-304, and the Spanish Ministry of Science and Innovation (MICINN) under Project No. MAT2009-07980. J.A.A. acknowledges MICINN for Fellowship No. BES-2010-035194. O.I. acknowledges the Basque Government for Fellowship No. BFI09.284.

- ¹A. Moser, K. Takano, D. T. Margulies, M. Albrecht, Y. Sonobe, Y. Ikeda, S. H. Sun, and E. E. Fullerton, *J. Phys. D: Appl. Phys.* **35**, R157 (2002).
- ²S. N. Piramanayagam, *J. Appl. Phys.* **102**, 011301 (2007).
- ³Y. Shirosishi, K. Fukuda, I. Tagawa, H. Iwasaki, S. Takenoiri, H. Tanaka, H. Mutoh, and N. Yoshikawa, *IEEE Trans. Magn.* **45**, 3816 (2009).
- ⁴R. Wood, M. Williams, A. Kavcic, and J. Miles, *IEEE Trans. Magn.* **45**, 917 (2009).
- ⁵I. Tudosa, C. Stamm, A. B. Kashuba, F. King, H. C. Siegmann, J. Stöhr, G. Ju, B. Lu, and D. Weller, *Nature (London)* **428**, 831 (2004).
- ⁶D. C. Ralph and M. D. Stiles, *J. Magn. Magn. Mater.* **320**, 1190 (2008).
- ⁷R. W. Chantrell, D. Weller, T. J. Klemmer, S. Sun, and E. E. Fullerton, *J. Appl. Phys.* **91**, 6866 (2002).
- ⁸H. Forster, T. Schrefl, R. Dittrich, D. Suess, W. Scholz, V. Tsiantos, J. Fidler, K. Nielsch, H. Hofmeister, H. Kronmuller, and S. Fischer, *IEEE Trans. Magn.* **38**, 2580 (2002).
- ⁹B. D. Terris and T. Thomson, *J. Phys. D: Appl. Phys.* **38**, R199 (2005).
- ¹⁰O. Hovorka, Y. Liu, K. A. Dahmen, and A. Berger, *Appl. Phys. Lett.* **95**, 192504 (2009).
- ¹¹A. Moser and D. Weller, *IEEE Trans. Magn.* **35**, 4423 (1999).
- ¹²A. Berger, A. Inomata, J. S. Jiang, J. S. Pearson, and S. D. Bader, *Phys. Rev. Lett.* **85**, 4723 (2000).
- ¹³A. Berger, D. T. Margulies, and H. Do, *Appl. Phys. Lett.* **85**, 1571 (2004); A. Berger, O. Hovorka, G. Friedman, and E. E. Fullerton, *Phys. Rev. B* **78**, 224407 (2008).
- ¹⁴O. Idigoras, A. K. Suszka, P. Landeros, P. Vavassori, J. M. Porro, and A. Berger, *Phys. Rev. B* **84**, 132403 (2011).
- ¹⁵O. Idigoras, P. Vavassori, J. M. Porro, and A. Berger, *J. Magn. Magn. Mater.* **320**, L57–L60 (2010).
- ¹⁶G. Choe, M. Zheng, B. R. Acharya, E. N. Abarra, and J. N. Zhou, *IEEE Trans. Magn.* **41**, 3172 (2005); G. Choe, J. Park, Y. Ikeda, B. Lengsfeld, T. Olson, K. Z. Zhang, S. Florez, and A. Ghaderi, *IEEE Trans. Magn.* **47**, 55 (2011).
- ¹⁷H. Katada, M. Hashimoto, Y. Urakami, S. Das, M. Shiimoto, M. Sugiyama, T. Ichihara, H. Hoshiya, K. Tanahashi, and K. Nakamoto, *IEEE Trans. Magn.* **46**, 798 (2010).